

Distributed Sensing Over Meter Lengths Using Twisted Multicore Optical Fiber with Continuous Bragg Gratings

*P. S. Westbrook^{*1}, K.S. Feder^{*1}, T. Kremp^{*1}, W. Ko^{*1}, H. Wu^{*1},
E. Monberg^{*1}, D. A. Simoff^{*2}, K. Bradley^{*3}, R. Ortiz^{*1}*

〈概要〉

本論文では、形状、温度、ひずみや音響信号などの様々な分散型感知用に、全長にわたってファイバブラッググレーティングを施したマルチコアファイバに関する最近の開発、および形状観測に適した集積型光ファイバ部品の説明を行う。この形状観測モジュールには周期的なねじりが加えられ、長手方向にブラッググレーティングが書き込まれたマルチコア光ファイバにて構成されている。このファイバは、1メートルあたり50回のピッチでねじりが加えられた被覆外径200ミクロンのコンパクトな光ファイバに0.001%/cm以上の反射率のグレーティングが施されており、数メートル以上のファイバの高効率な散乱測定に適している。このマルチコアファイバはFitel[®]製融着機を用いて融着可能なことも実証が行われている。このファイバに使用されているUV光を透過する被覆層は、被覆を除去することなくグレーティング書き込みを可能にしつつ、通常ファイバと同等の機械的強度を実現している。このファイバの反射光を利用した様々な形状を観測する実証が行われている。最後に、従来使用していたレイリー後方散乱光による方式よりも、広帯域に連続的なレイリー散乱状後方散乱光を発生させることのできるファイバを使用した分布型のひずみ、温度、音響センサーについて報告する。

1. INTRODUCTION

Optical fiber sensors are attractive for a number of industrial and medical applications that exploit the unique advantages of optical fiber. These include compact, lightweight, in-fiber design, optical multiplexing capabilities, and resistance to harsh temperature, chemical and radiation conditions as well as freedom from electromagnetic interference. As such they have found application in various industries that benefit from distributed sensing, such as the oil and gas industry and structural health monitoring. Recently, there has been increased interest in next generation fiber sensors with enhanced capabilities that exploit advances in multicore fibers and continuous array fabrication. These include distributed temperature¹⁾, strain²⁾ and acoustic sensing³⁾, as well as sensing of bend and shape^{4), 5)}. Such applications often require continuous or nearly continuous sensing along the length of the fiber. While Rayleigh scattering can provide a spatially continuous sensing signal^{1), 2)}, it has limitations due to low signal intensity and the inherent randomness of the Rayleigh scattering spectrum. Distributed sensing applications can thus benefit from the increased elastic scattering and well controlled optical spectra of continuous intra-core Bragg gratings. In addition to the requirements

of continuous sensing, some applications, such as shape sensing, also require multicore fibers. Offset cores in such fibers provide information about the state of bend and twist of the fiber such that sensing signals from these cores can be used to reconstruct the shape of an optical fiber.

A critical requirement for these applications is a cost effective method to fabricate continuous arrays of gratings over many meters in all of the cores of a multicore fiber. We have recently reported on a fabrication system suitable for long continuous multicore sensor arrays^{6), 7)}. Our method uses reel to reel fiber handling and UV transparent coating, and is both flexible, allowing control over the local grating spectrum, as well as scalable, allowing for arbitrary lengths of nearly continuous arrays to be inscribed in all cores of a fiber. Without removal of the fiber coating, near pristine fiber mechanical strength is maintained.

In this work we report on continuous fiber grating arrays suitable for sensing applications. We describe the properties and fabrication of nearly continuous single frequency grating arrays in twisted multicore fiber suitable for fiber shape reconstruction in medical instruments. We also demonstrate the bend sensing capability of the fiber by performing shape reconstruction. We then show that a broadband enhanced scattering spectrum may be imprinted in all of the cores simultaneously. Such grating arrays act as enhanced Rayleigh-like scattering waveguides and can improve signal to noise in various sensing

^{*1} OFS Fitel, LLC, Somerset, NJ, OFS Laboratories

^{*2} OFS Fitel, LLC, Avon, CT

^{*3} OFS Fitel, LLC, Norcross, GA

applications such as distributed temperature, strain, and acoustic sensing.

Our review is organized as follows: We first provide background on the optical requirements for shape sensing. We first review the principals of optical fiber shape sensing. We discuss optical interrogator units used to characterize sensor performance and also used in the final shape sensing application. We then describe the different components of our optical fiber shape sensor, including the twisted optical fiber, multicore fiber splicing, grating arrays, connectorization, and multicore fanouts. We then demonstrate the shape sensing capability of our arrays by performing a shape reconstruction. Finally, we describe continuous broadband gratings suitable for sensing of temperature, strain and acoustic signals.

2. SHAPE SENSING BACKGROUND

Shape sensing using optical fibers exploits the strain sensitivity of light propagating in an optical fiber waveguide core^{4), 5)}. When such a core is offset from the center of a fiber it experiences a strain that depends on both the bend radius and bend direction of the fiber. By using more than one offset core, the direction of the bend may be determined. A center core may also be added to sense thermal and longitudinal strain variations. When such a multicore fiber is twisted, the outer cores will all be strained in the same way, while the neutral axis, which is very close or identical to the optical axis in the center of the fiber, remains unstrained. To differentiate between left handed and right handed twist, a permanent twist may be added to the outer cores. A fiber design that satisfies these requirements has twisted offset cores at equal radius surrounding a central core. See Figure 2 and Figure 3.

Accurate shape sensing requires knowledge of the state of strain with very high spatial resolution. Therefore, the strain must be measured continuously, or nearly continuously along the entire fiber length. Such a measurement is most easily performed if there is a very weak Bragg grating along the entire length of the optical fiber. A Bragg grating is a periodic modulation of the refractive index along the core of an optical fiber. Such a grating reflects core guided light at a wavelength λ_{Bragg} determined by the Bragg condition:

$$\lambda_{Bragg} = 2n_{eff} \Lambda_{grating} \quad (1)$$

where n_{eff} is the effective index of the guided mode and $\Lambda_{grating}$ is the period of the grating. For gratings in typical germanosilicate single mode fibers, a Bragg resonance wavelength in the telecom band near 1550 nm requires a grating period on the order of 500 nm. When the fiber is strained by an amount ε , the Bragg resonance of the grating is shifted spectrally by an amount $\delta\lambda_{Bragg}$ given by

$$\frac{\delta\lambda_{Bragg}}{\lambda_{Bragg}} = k\varepsilon, \quad (2)$$

where $k \approx 0.78$ is determined by the photoelastic response of the waveguide material. Thus, measurements of the local Bragg period of gratings in each core can be related to the local state of strain in each core. If the cores are transversely located at known offset positions, then the strain state of the fiber may be related to the local fiber bend magnitude and direction as well as the twist. As the strain in each core is changed, this spectral characteristic will shift much like a Bragg grating spectrum shifts under fiber strain.

Once the local strain and twist are known, the shape of the fiber may be computed using geometric formulations such as the Frenet-Serret equations that relate local curvature and twist to the evolution of a local coordinate system that tracks the fiber tangent⁶⁾. These equations may be written as

$$\frac{d}{ds} \begin{bmatrix} T \\ N \\ B \end{bmatrix} = \begin{bmatrix} 0 & \kappa & 0 \\ -\kappa & 0 & \tau \\ 0 & -\tau & 0 \end{bmatrix} \begin{bmatrix} T \\ N \\ B \end{bmatrix}, \quad (3)$$

where T , N , and B are the tangent, normal, and binormal vectors at a given point s along the optical fiber and ds is an increment of length along the optical fiber. The quantities κ and τ are the local curvature and twist, respectively. These geometrical parameters are obtained from the local strain measurement at the multiple cores using the observed shifts in Bragg wavelength for each core.

3. SENSOR MEASUREMENT AND OFDR

The grating array may be measured using a variety of optical interrogation methods. In typical fiber Bragg grating sensor applications, strain is measured by recording the shift in the Bragg grating spectrum using an optical spectrum analyzer. The spatial resolution of such an approach is limited by the length of the grating, typically greater than 1 mm. To obtain information continuously along a length of meters requires multiplexing of many sensors. Traditional wavelength and time domain multiplexing schemes have limitations on the spacing and number of gratings that generally preclude their use in continuous measurement of strain along a 1 m length of fiber with the sub mm spatial resolution required for shape sensing.

A more suitable interrogator for the high resolution local strain uses the technique of optical frequency domain reflectometry (OFDR). Such spectral interferometry may be performed with commercial instruments such as the LUNA OBR. We describe this technique here because it can be used as an interrogator for distributed shape, temperature and strain sensing, but also because OFDR is the desired test method used to characterize the performance of our long, weakly reflecting sensor gratings.

Figure 1 shows a schematic of such a system. In OFDR, a narrow band laser signal is coupled into the fiber and the reflected light is collected and interfered with a

reference signal that experiences a single back reflection. The laser is scanned over a given frequency range from ν to $\nu+\Delta\nu$ to yield a spectrum in which the reflected light has a spectral beat term between the reference and the sensor grating reflections. This beat term oscillates as a function of the laser frequency detuning $\Delta\nu$:

$$P(\nu+\Delta\nu) = |E_{ref} + E_{sensor}|^2 \sim \text{Re} \sum_{z_i} E_{ref} R_i(\nu+\Delta\nu) \exp\left\{2j\left(k(\nu) + \frac{2\pi\Delta\nu n_{group}}{c}\right)(z_i - z_{ref})\right\} \quad (4)$$

where the sum is over all points z_i along the fiber, $R_i(\nu)$ is the frequency dependence of the reflection of the increment at z_i , $k(\nu) = 2\pi\nu n_{eff}(\nu)/c$, n_{group} is the group index, and we assume that the effective and group indices are the same in both paths. Thus, each point along the sensor contributes a term to the OFDR frequency trace that oscillates vs frequency with a period that is proportional to its position along the fiber. Thus, a Fourier transform of $P(\nu+\Delta\nu)$ will give the spatial dependence of the amplitude and phase of the light scattered from each point in the fiber:

$$R(z_i) \sim FT\{P(\nu+\Delta\nu)\} \quad (5)$$

The intensity of the reflection is then simply $|R(z_i)|^2$. If a Bragg grating is present, the spatial phase of the back reflected light will be determined largely by the grating. The derivative of this spatial phase can then be related to a local Bragg wavelength $\lambda_{Bragg}(z_i)$ through:

$$k_{Bragg}(z_i) = \frac{2\pi n_{eff}}{\lambda_{Bragg}(z_i)} = \frac{d\text{Arg}\{R(z_i)\}}{dz}, \quad (6)$$

where $\text{Arg}\{R(z_i)\}$ is simply the spatial phase of the reflected light and n_{eff} is the mode effective index. Thus, when a given core experiences a change in strain, the value of the spatial phase derivative at that point will change. The spatial resolution of the OFDR technique depends on the wavelength scan range $\Delta\nu$. The larger the wavelength scan range, the finer the spatial resolution. A typical value would be a 20 nm scan near 1550 nm, and this would give a spatial resolution of approximately 40 μm . Such fine resolution is a significant driver for the use of OFDR and continuous gratings in shape sensing where positional resolution is very important to ensure accurate shape reconstruction. This accuracy cannot be obtained using discrete Bragg gratings in schemes that use spectroscopic or wavelength division multiplexed (WDM) or time domain (TDM) interrogators. Moreover, OFDR can also be used to measure fiber strain with Rayleigh scattering, making this approach quite versatile. The primary disadvantages of the technique are the stability and data handling requirements since it is an interferometric technique, and the large quantity of data limits the speed of the method and increases the cost of the interrogator. It is also less effective with strong back reflectors due to multipath interference, in particular for

very long grating arrays. However, as a diagnostic technique using weak Bragg gratings and Rayleigh scattering, OFDR is superior to other methods. Therefore we present OFDR traces of our devices in the work shown below.

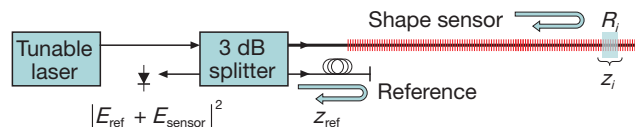


Figure 1 Schematic of Optical Frequency Domain Reflectometry (OFDR) system used for high spatial resolution measurement and interrogation of distributed sensors.

4. SHAPE SENSOR OPTICAL ASSEMBLY

In order to satisfy the demand for accuracy, small size, and cost we have developed a set of components based on twisted multicore fiber technology. A schematic of our shape sensor optical assembly is shown in Figure 2.

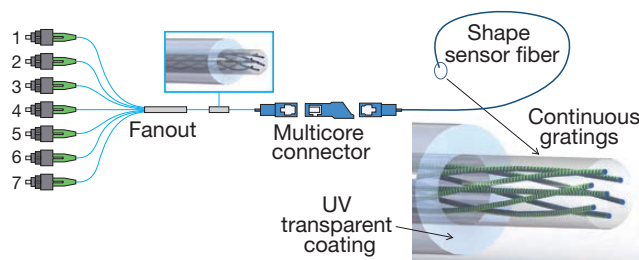


Figure 2 Multicore optical fiber shape sensor assembly, including a fanout that combines single core fibers and couples them to the multicore fiber, multicore connectors and jumpers, and the twisted continuous fiber Bragg grating sensor array. A schematic of the twisted multicore grating array that comprises the shape sensor head is also shown. UV transparent coating protects the fiber while allowing for flexible, high volume fabrication of shape sensor arrays.

Figure 3 shows a cross section of a multicore optical fiber used for the sensor, fanout and jumpers. Six cores surround a center core at the neutral axis of the fiber. Only three of the outer cores are necessary for shape sensing. The other three give added flexibility and redundancy in manufacturing and can improve sensor performance. The fiber has a 125 μm outer diameter and a 35 μm core-to-core spacing. The fiber is coated with a UV transparent coating that ensures fiber strength while allowing grating inscription using standard methods as described below. The cores have a typical numerical aperture (NA) of 0.21. This NA improves grating inscription, and improves bend loss immunity, while maintaining acceptable connector and splice losses. Importantly, the core positions are accurate to below 0.75 μm and the effective indices of the cores are matched to within 0.05%. These tolerances improve the accuracy of the resulting shape sensor and make the Bragg resonance of

the gratings highly repeatable between cores. A permanent twist is imposed on the fiber during the draw process by spinning the preform at a high rate. The typical twist is 50 turns per meter, which is equivalent to a twist pitch of 2 cm.

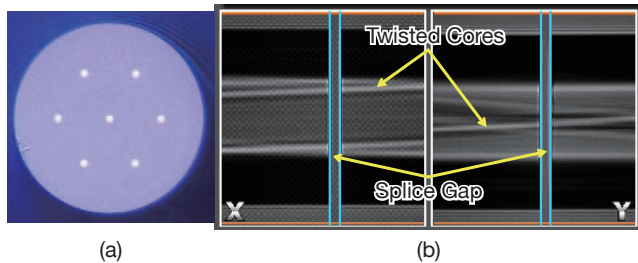


Figure 3 (a) Cross section of a twisted multicore fiber (MCF) used throughout the optical fiber shape sensor assembly of Figure 2. (b) Side view of a twisted fiber as seen from two orthogonal directions (x,y) in the Fitel S183 PM II fusion splicer. Twist of the fiber cores is evident in the angled image of the outer cores. The Fitel splicer algorithm has automatically aligned the twist across the gap between the two fibers before performing the splice. Dark regions result from fiber lensing.

Another important component needed for testing the MCF is an effective splicer that can align multiple cores as well as twist phase during the splicing alignment. We have adapted the splicing routines on the Fitel S183 PM II Fusion Splicer to obtain optimized splices for both twisted and untwisted MCF with seven cores. Figure 3 (b) shows orthogonal side views of two twisted multicore fibers that have been aligned with respect to each other.

Figure 4 shows a schematic of the grating inscription apparatus used to write the quasi-continuous Bragg gratings that make up the sensor array. This process exploits an acrylate based UV transparent fiber coating that protects the optical fiber to maintain its mechanical strength at near pristine levels while at the same time allowing for UV inscription of gratings using well known inscription methods. A precision encoder allows control of gaps between gratings to less than 1 mm. This spacing is on the order of the spatial resolution required for many shape sensing applications, making these grating arrays effectively continuous sensing arrays. The inscription allows for parallel fabrication of gratings in all cores with a single shot exposure at each location along the fiber. An example of a 2 m long grating is shown in Figure 5. For clarity, only the center core signal is shown. The grating exhibits a reflection level 25 dB above the Rayleigh scattering background. This enhancement in backscattering signal is one of the key benefits of using Bragg gratings for distributed sensing applications. The inset shows the local spectrum from 1 cm of grating. A sharply peaked spectrum is observed indicating a well-defined Bragg resonance. The sharply peaked spectrum of the grating is also evident in the local Bragg wavelength, which is the inverse of the spatial derivative of the reflection phase

(see Eq. 6), and is therefore commonly referred to as “phase derivative” (red line). This shows a well-defined Bragg resonance near 1542 nm that is maintained over the 2 m length. The clearly defined spectral feature and phase derivative is also highly desirable for shape sensing since the algorithms used to track the phase simply rely on changes in local Bragg period. The plot also shows a 3 dB increase in signal at the splice between the input standard single mode fiber (SSMF) and the multicore fiber (MCF). This increase is consistent with the core design which was intended to have a larger Rayleigh scattering signal than SSMF. Note that in the Rayleigh scattering region, the phase derivative is quite noisy compared to the FBG. This is expected since Rayleigh scattering results from random perturbations of the refractive index. Despite this noise, the Rayleigh scattering can also be used to obtain the shape of the fiber, however at the cost of processing speed and complexity. The 3 dB increase in scattering resulting from our fiber design then improves the performance of our fiber for Rayleigh based sensing as well. Note that while the example in Figure 5 shows a weak, fixed FBG period meant for OFDR interrogation, the flexibility of our writing apparatus would allow for a more conventional set of stronger discrete Bragg gratings at a range of wavelengths that would be suitable for wavelength division multiplexed (WDM) interrogation of our sensor array.

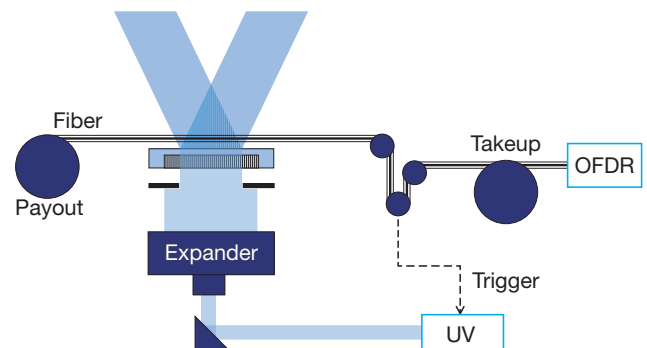


Figure 4 Continuous fiber grating fabrication apparatus employing UV transparent coated fiber and precision encoders to achieve effectively continuous gratings along any length of fiber.

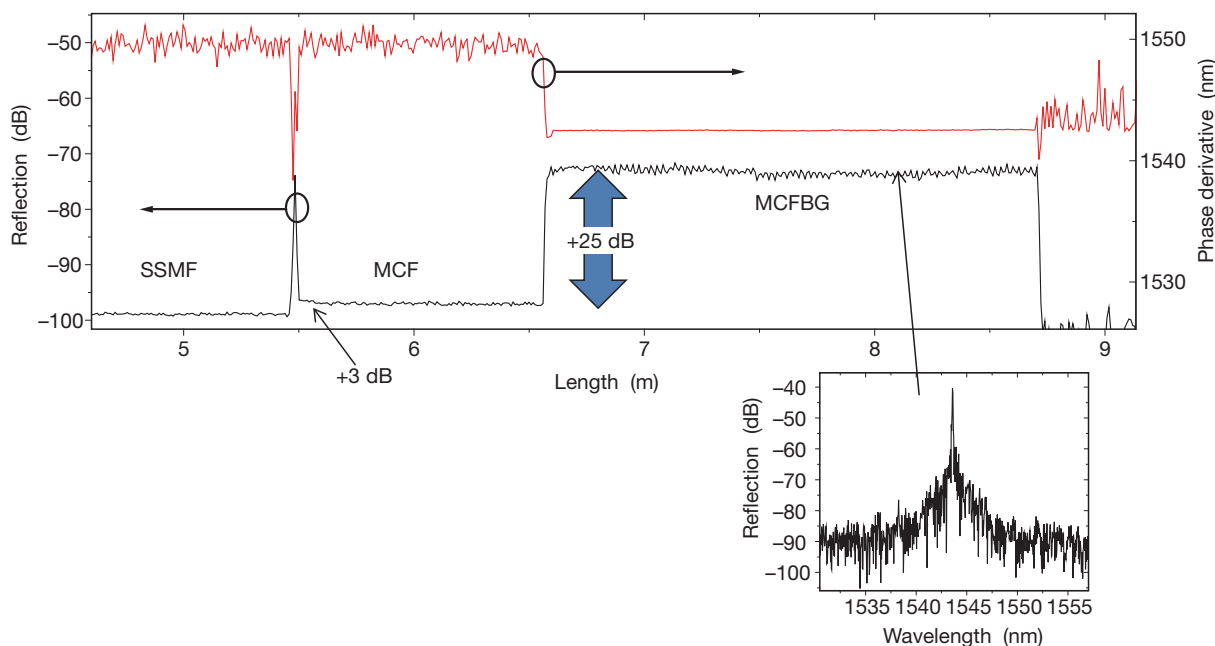


Figure 5 OFDR (LUNA OBR) trace of a 2 m long continuous FBG array. The black curve shows the reflected intensity as a function of position. A clear jump in the Rayleigh scattering intensity is observed at the splice from standard single mode fiber (SSMF) to the multicore fiber (MCF) near 5.5 m. A 25 dB increase in signal is observed near 6.6 m where the multicore FBG (MCFBG) begins. The red curve shows the local Bragg wavelength, which is inversely proportional to the spatial phase derivative. In the Rayleigh scattering region, the phase derivative is very noisy, while within the Bragg grating very little noise is observed. The inset shows the spectrum extracted from a 1 cm section within the grating.

5. SHAPE RECONSTRUCTION

In order to demonstrate the sensing capability of our shape sensor fiber, we performed shape reconstruction demonstrations. A length of twisted multicore fiber grating array was fabricated using the system shown in Figure 4. This fiber was then measured using an OFDR system as shown in Figure 1. The fiber was first measured in a straight, unstrained and untwisted configuration. This measurement was then used as a reference to

obtain the local bend and twist of the fiber along its entire length. These measurements were then used to reconstruct the shape of the optical fiber. Our results are shown in Figure 6. The fiber was wrapped around spools of different diameters. OFDR measurements were performed on four different cores and the shape reconstruction technique of section 2 and REFERENCE 8) was applied to reconstruct the shape of the fiber from the OFDR traces. The results are shown in Figure 6 (a) and Figure 6 (b). In another experiment, the fiber was wrapped around a post

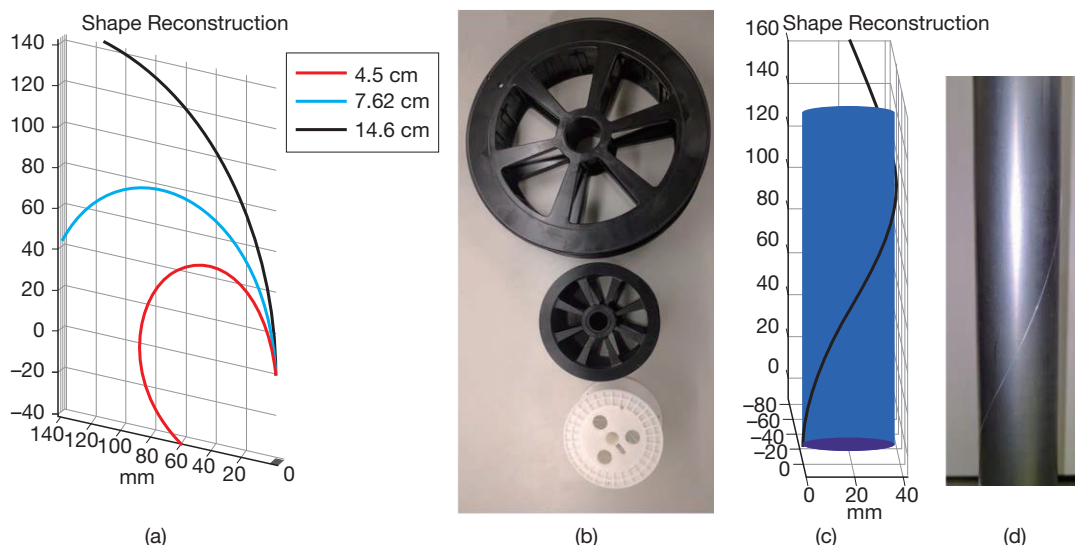


Figure 6 Demonstration of shape reconstruction described in section 2. (a) Reconstructed shape of fiber bent around spools shown in (b). (c) Shape reconstruction of a fiber wrapped around a post as show in (d).

after the reference scan was performed. Figure 6 (c) and 6 (d) show the reconstructed fiber shape and a photo of the fiber wrapped around the post. This demonstration shows the capabilities of the shape sensing fiber. Such shape reconstruction is useful in any application that requires position and/or shape information, particularly those in which other position measurement methods fail, such as medical procedures using catheters, underground measurements without GPS, measurements in environments with harsh temperature, chemical or radiation conditions, and applications with significant electromagnetic interference.

6. CONTINUOUS BROADBAND ENHANCED SCATTERING FIBER

Another important application of our technology is continuously enhanced scattering fiber. Such fiber can provide additional signal in applications that rely on scattering from optical fiber. These include distributed temperature, strain and acoustic sensing that use Rayleigh backscattering. Figure 7 (a) and 7 (b) show an example of a 2 m

long grating in a multicore fiber that exhibits more than 20 dB enhanced scattering in the inner and outer cores. Such enhanced scattering can improve signal to noise in various applications that require increased scattering signal. One such application is distributed temperature sensing that uses broadband scattering. It is well known that OFDR can be used with Rayleigh scattered back reflection in a fiber waveguide to measure the change in temperature along the fiber^{1), 2)}. The same continuous and high precision measurement may be achieved for temperature variations as was described for strain in the shape sensing application. A limitation of such measurements is that Rayleigh scattering is very weak. As a result, loss due to fiber attenuation or connectors can prevent the use of Rayleigh scattering. As shown in Figure 7, the use of gratings can increase the scattering by as much as two orders of magnitude. As a result, temperature sensing capability can be maintained even in the presence of very large loss. One such example was shown in REFERENCE 9) in which a 10 dB connector (20 dB round trip loss) loss was overcome in a distributed temperature sensing application by using a continuous broadband grating

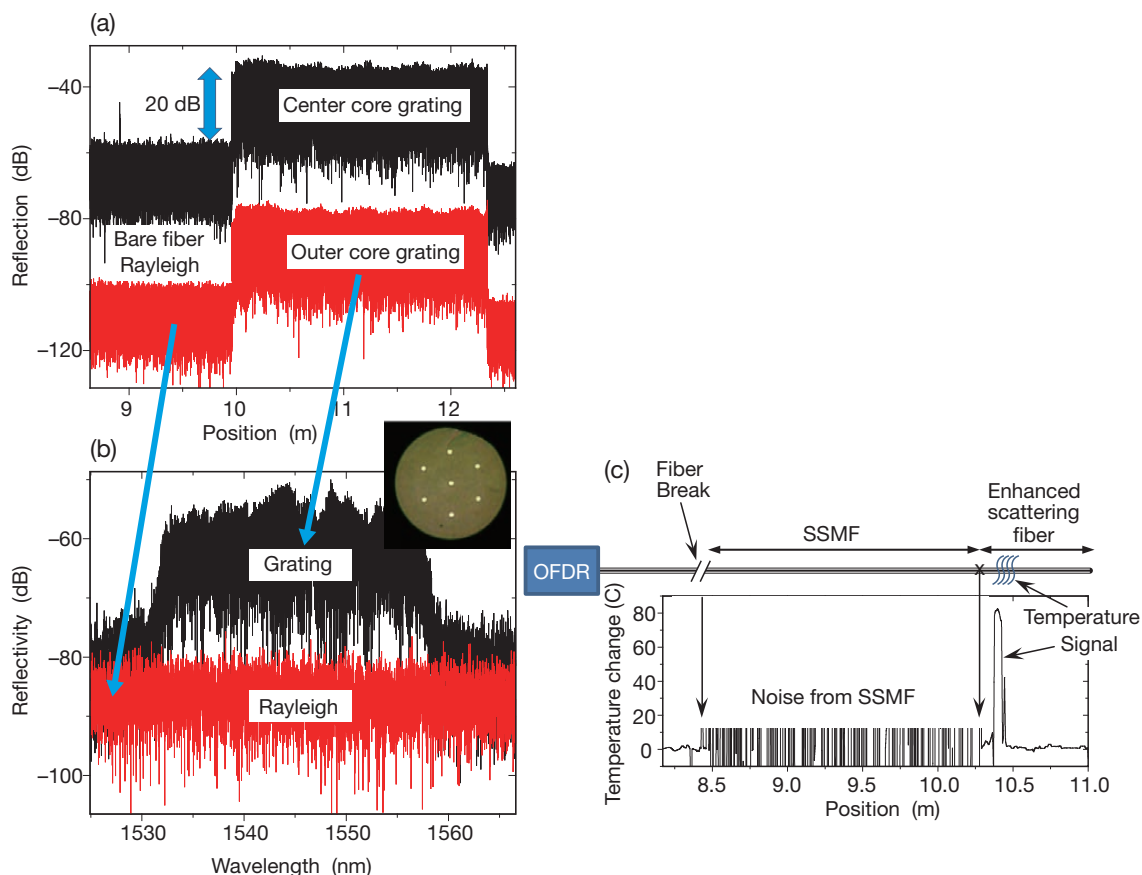


Figure 7 (a) OFDR Reflection vs position measured for an inner and one outer core of the twisted multicore fiber with broadband enhanced scattering array. Multicore fiber cross section shown in the inset. A single UV inscription exposure using the setup of Figure 4 increases scattering at all locations and in all cores. (b) OFDR derived spectrum taken from a position within the grating (11 m) and in the bare fiber (9.5 m), showing more than 20 dB increase in signal over the Rayleigh scattering of the bare fiber core. (c) Demonstration of enhanced signal to noise using broadband enhanced scattering fiber. The experimental setup is shown on the top. The OFDR interrogator sends signals into the sensing fibers. A fiber break between the OFDR and the sensor fibers results in large loss (10 dB). The standard single mode fiber (SSMF) gives only noise. The enhanced scattering fiber with continuous gratings is still able to record a temperature variation and return the sensing information to the OFDR interrogator through the large loss at the fiber break.

enhanced back scattering fiber. Figure 7 (c) shows the OFDR interrogator coupled to two distributed temperature sensors through the 10 dB loss at the fiber break. The standard single mode fiber (SSMF) yields only a noisy signal due to its low Rayleigh back scattering signal. The broadband enhanced scattering fiber, though, provides a signal that the OFDR is able to convert to the local temperature distribution. In this example the temperature is uniform everywhere except for the short section indicated where a heater has increased the temperature.

In practice, such scattering fibers can be fabricated using the setup shown in Figure 4. Typically, the single frequency, uniform period Bragg grating can be replaced with a broadband chirped fiber grating by using a different phase mask. For instance a chirped phase mask may be used to obtain a broadband reflection over many nm at telecom wavelengths.

By providing some overlap from one grating to the next it is possible to obtain a spatially continuous broadband back reflection. We note that such a grating no longer has the clear, easily interpreted spatial phase derivative signal of the uniform Bragg grating. However, the algorithm of REFERENCE 2) can be applied to a partially or completely random spectral phase and amplitude signature. As a result, such broadband gratings may provide a greater signal, while still allowing the sensor algorithm to function.

7. CONCLUSION

We have discussed the properties and applications of long, continuous optical fiber sensor arrays suitable for various distributed sensing applications that require continuous high precision measurement. These include sensing of fiber shape, temperature, strain and acoustic signals. For optical fiber shape sensing we have developed a set of optical components suitable for shape reconstruction applications in medical, industrial, and other applications. These include twisted optical fiber with multiple cores, multicore fiber splicing, fiber gratings for increased scattering efficiency, multicore connectors and jumpers, and single core to multicore fanouts. Our components are aimed particularly at medical applications that require robust, compact, high speed and highly accurate measurements. Connectorized parts allow end users the flexibility to configure the sensor for many applications. Our sensors can be fabricated with grating arrays suitable for interrogation schemes beyond OFDR, including wavelength and time division multiplexed systems. For other distributed sensing applications such as strain, temperature and acoustic sensing, we also describe enhanced scattering fiber that can greatly increase signal to noise for various sensing applications.

REFERENCES

- 1) Gifford, Dawn K., et al. "Distributed fiber-optic temperature sensing using Rayleigh backscatter." *ECOC Proceedings*. Vol. 3. 511-512, 2005.
- 2) M. Froggatt et al., "High-spatial-resolution distributed strain measurement in optical fiber with Rayleigh scatter", *Appl. Opt.* 37, 1735-1740 (1998).
- 3) Daley, Thomas M., et al. "Field testing of fiber-optic distributed acoustic sensing (DAS) for subsurface seismic monitoring." *The Leading Edge* 32.6 (2013): 699-706.
- 4) M. J. Gander, et al., "Bend measurement using Bragg gratings in multi-core fiber", *Electron. Lett.* 36, 120-121 (2000).
- 5) R. G. Duncan, et al., "High accuracy fiber-optic shape sensing", *Proc. SPIE* 6530, 65301S-11 (2007).
- 6) P. S. Westbrook, et al., "Integrated optical fiber shape sensor modules based on twisted multicore fiber grating arrays", *Proc. SPIE* 8938, 89380H (2014).
- 7) P. S. Westbrook, et al., "Multicore optical fiber grating array fabrication for medical sensing applications", *Proc. SPIE* 9317, 93170C (2015).
- 8) J. P. Moore and M. D. Rogge, "Shape sensing using multi-core fiber optic cable and parametric curve solutions", *Optics Expr* 20 2967-2973 (2012).
- 9) P. S. Westbrook, T. Kremp, K. S. Feder, T. F. Taunay, E. Monberg, R. Ortiz, "Grating enhanced back scatter fiber for distributed sensing", *CLEO 2016*, paper STu4H.4, (2016).